Nutation Aids Heterogeneous Substrate Exploration in a Robophysical Root

Yasemin Ozkan-Aydin[1], Mason Murray-Cooper[1], Enes Aydin[1], Erin N. McCaskey[1], Nicholas Naclerio[2]
Elliot W. Hawkes[2] and Daniel I. Goldman[1]

Abstract— **For exploration of unknown terrestrial environments, it is typically assumed that robots possess sophisticated controllers which can sense important aspects of the terrain (gaps, obstacles, slippery surfaces). However, robust sensing of such conditions is not yet possible in harsh environmental conditions. Biological systems, including plant roots and snakes, are impressive in their ability to use diverse growth and movement strategies to penetrate and explore heterogeneous terrain. Such systems avoid becoming trapped, despite lacking full terrain state information. We are particularly interested in how circumnutation – an endogenous circular pattern exhibited by the tip of a growing root – facilitates penetration and exploration. To discover principles by which robots can gain root-like capabilities, we constructed a planar, pneumatically driven soft-bodied robot, which grows from the tip like a plant root and can bend in 2D space by oscillating the inflation pressure of series pneumatic artificial muscles (sPAMs) arranged on its two sides. We demonstrate that 2D tip oscillation improves the robotic roots ability to penetrate a heterogeneous environment, tested in a lattice of rigid cylinders distributed evenly on a square board. Systematic variation of initial robot positions revealed that the non-oscillating tip strategy led to an increased probability of becoming pinned to obstacles (and preventing growth), while the oscillating tip penetrated the lattice significantly further. The results show that without closed loop control, oscillatory movements of a leading surface of a growing structure enable robust navigation in a heterogeneous environment; closed loop control strategies layered on top of such passive mechanisms could lead to novel strategies for exploratory and search-and-rescue robotics.**

I. INTRODUCTION

In extreme terrains and operating conditions such as search-and-rescue operations, robots should be capable of effectively navigating in complex landscapes, handling failures and adapting to the environment. This usually requires significant levels of autonomy supported by sensory feedback [1]. During the last few decades researchers have built search-and-rescue robots based on biological models which effectively move in unstructured environments [2], [3]. The snake-like robot (Fig. 1A) consisting of a series of 18 independent modules that are connected and programmed to work together can navigate through cluttered terrain using a continuously-active feedback controller that relies heavily on on-board sensors at each link [2]. Recently, a root-inspired

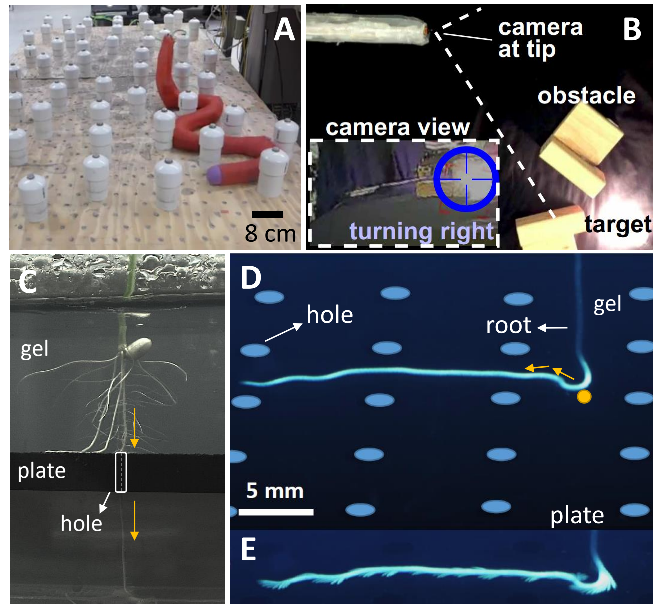

Fig. 1. **Biological and robotic models that explore environment.** (A) A snake-like robot moves through obstacles with a complex, active control scheme [2]. (B) A growing robot navigates its environment using a tip-camera [3]. (C) A circumnutating rice root explores its environment. The root is growing along a plate with a grid of holes spaced 7mm apart in gel; a circumnutating tip finds the hole on the plate and grows longer (the direction of growth shown by arrows). (D) A root tip touches a plate from the point labeled with yellow circle and oscillates along the surface [4]. (E) Maximum intensity projection of the circumnutating root tip from B showing the oscillatory movement along the surface. Images were taken every fifteen minutes for a period of five days.

robot (Fig. 1B) that grows through an obstacle course using a vision sensor successfully navigates through restricted spaces [3]. However, in real-world situations, the sensor performance of the robots is affected by environmental conditions (dust, moisture, heat, etc.) resulting in unreliable sensory input for active control. Further, the sensors used for navigation are often large and expensive and require large amounts of power; this in turn reduces the mobility, dexterity and endurance and applicability of the robots [1].

Circumnutation is a natural plant movement which results in an oscillating growth pattern and is widespread among plants [5]. Recently researchers discovered that circumnutation promotes surface exploration and penetration by rice roots [4] (Fig. 1C-E). This study grew both circumnutating and non-circumnutating rice roots on plastic surfaces with a grid of holes of different densities in a gel environment and measured the success rate of the roots finding a hole. The roots that circumnutated at the tip had a higher success rate in

[1]Yasemin Ozkan-Aydin*, Mason Murray-Cooper, Enes Aydin, Erin McCaskey, and Daniel I. Goldman with the School of Physics, Georgia Institute of Technology, GA, USA. yasemin.ozkanaydin,and daniel.goldman @physics.gatech.edu

[2]Nicholas Naclerio and Elliot W. Hawkes with the Department of Mechanical Engineering, UC Santa Barbara, USA. nnaclerio@ucsb.edu, and ewhawkes@ucsb.edu

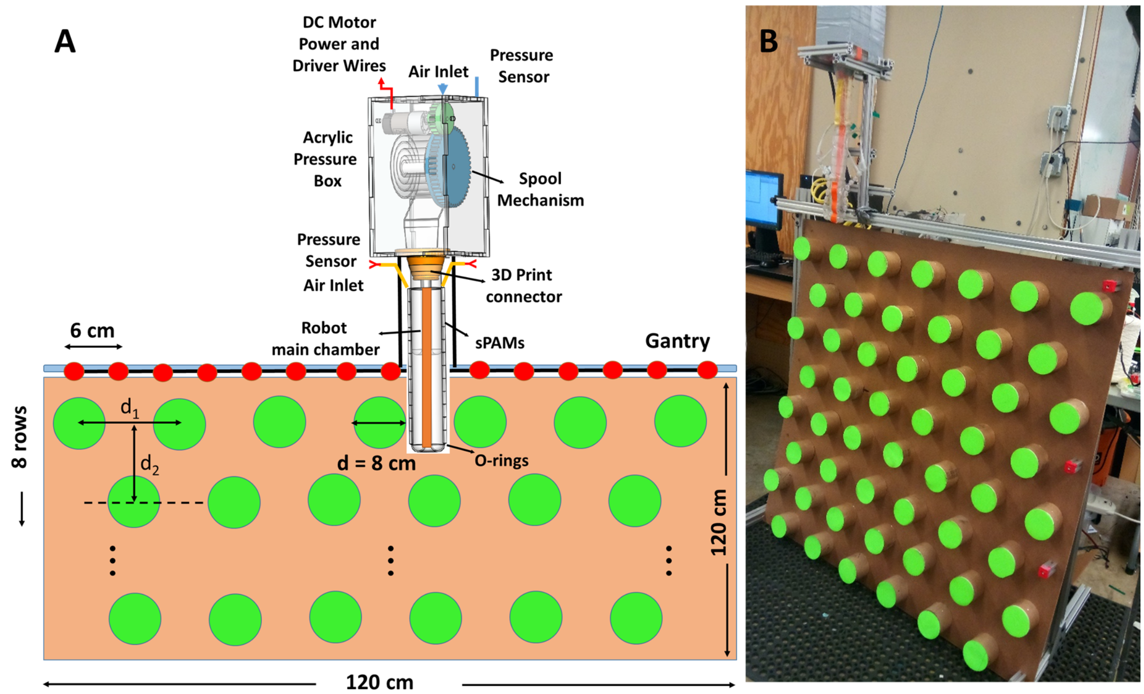

Fig. 2. **Growing robot and spool mechanism.** The sPAMs are attached the side of the main body with double-sided tape.The robot is mounted the bottom side of the laser cut acrylic (5mm thickness) pressure box. The spool mechanism driven by DC motor simultaneously winds/unwinds the growing part of the robot during tube expansion/rewinding. The cylindrical pegs (d=8 cm, height is 6.5 cm) are mounted on a particle board (120×120 cm) with a horizontal, d_1 and vertical, d_2 distance are 18 cm. The pressure box and the robot are placed on a horizontal gantry. The evenly distributed red dots represent the initial position of the robot during the experiments. The distance between two adjacent starting position is equal to 6 cm. (b) Physical setup.

finding a hole, for all hole densities, and consequently grew deeper in the gel. This inspired the idea that circumnutation could help as a passive strategy for movement in complex terrain.

Within the past few years, several groups have taken a soft robotic approach to test hypotheses of root growth [6], to discover functional benefits of circumnutation [7], and to develop novel exploratory devices [3], [8], [9]. Such robots differ from conventional locomoting devices in that they grow from the tip, mitigating body drag effects. For example, Mishima et al. developed a growing robot that uses a variant of tip eversion and showed that the robot can navigate in an unstructured environment such as rubble spaces [8]. Inspired by natural organisms that cover distances by growing (as opposed to locomoting as a unit), [3] built a lightweight soft continuum robot and developed control schemes through various obstacles using feedback from a camera located at the tip. A robot that builds its own body through an additive manufacturing process was created by [10] and its penetration capabilities were measured in a homogeneous granular medium; circumnutation of the tip reduced penetration forces.

In this paper we take a robophysical approach [11], [12] and systematically study the dynamics of a soft growing robot [9] which can use passive strategies to traverse a heterogeneous environment. Different from the previous robots [3], [13] (see Fig. 1C) that navigate through constrained environments using feedback mechanisms (camera, sensors etc.) and change the growing direction according to stimuli or often rely on continuously active sensing/control to locomote moving through obstacles (see Fig. 1D) [2], we demonstrate that simple tip oscillation improves penetration of the robot, enabling traversal of a laboratory heterogeneous environment without any feedback control.

II. EXPERIMENTAL SETUP

Our design is similar to the soft continuum robot previously built by [3], [8], [9]. Here we will explain the details of the setup we used in systematic experiments.

A. Robot

The robophysical root model shown in Fig. 2 was built by two different widths of lay-flat poly tubing (w_1= 7.5 and w_2= 2.5 cm, Hudson Exchange). The ratio between $w_1/w_2 = 3$ was chosen so that the inflated diameter of the body tube is greater than twice the inflated diameter of the side actuators to provide enough space for the inverted material stored inside the body. The total length of the robot is about 1m with an extra 1.5 m of material which is stored on a spool mechanism for tip extension. To make the poly tube airtight, one end is sealed with an impulse sealer and the sealed end is fed into the body. When pressure is applied, the material stored inside the body everts and the robot elongates from the tip. During eversion, the previously elongated part of the body does not move relative to the environment, which causes low friction with the outside [3]. To generate oscillations at the tip we use a series pneumatic artificial muscle (sPAM) that consists of multiple PAMs in series [14].

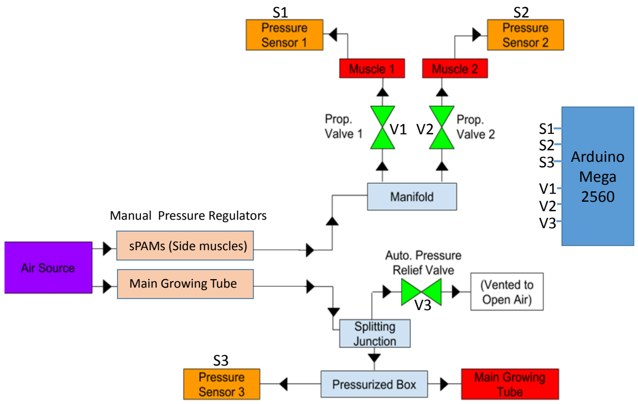

Fig. 3. **The pneumatic control circuit**. The control circuit includes manual pressure regulators, two proportional valves, one 2-way auto relief valve, pressure sensors and Arduino Mega 2560 micro-controller.

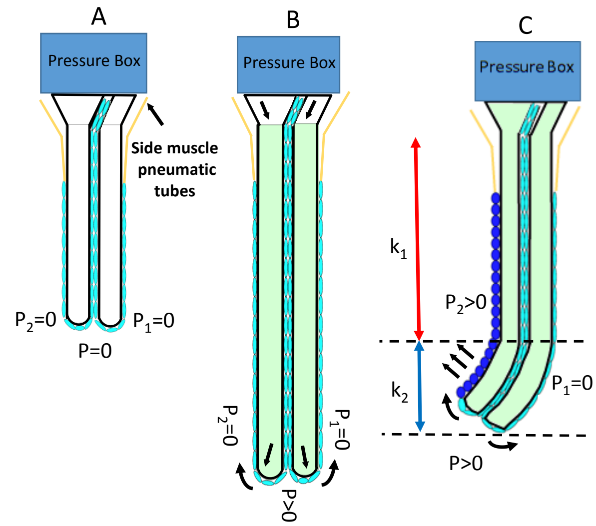

Fig. 4. **Diagram of tip eversion based growth and steering.** (A) Initial configuration of the robot when all the muscle pressures (body, P and sPAMs, P_1, P_2) are zero. (B) The robot grows from its tip when the main body tube is pressurized ($P > 0$ and $P_1, P_2 = 0$), the direction of the elongation is parallel to horizontal plane. (C) The robot bends left when the sPAM on that side is activated ($P_2 > 0$). The pressure of the main body is higher when it is close to the pressure box and the stiffness of the inflated tube $k_1 > k_2$, which helps the tip bend more than the upper body.

The sPAMs are made of 2.5 cm diameter lay-flat poly tubing with O-rings (d= 4.5 mm, durometer 90A) placed around the tube every 2 cm. The sPAMs are attached to two sides of the body with double-sided tape (iCraft Supertape, Amazon). The overall motion of the side actuators is controlled by modifying the geometry of the individual chambers through pressure. When the sPAMs are inflated, the tube between o-rings distends, and the overall length of the actuator shortens resulting in bending to that side. We used colored tape along the main body of the robot for image processing.

B. *Pressure Box*

To wind and unwind the backbone of the robot while keeping the pressure sufficient for growing we used a custom acrylic (w= 6.35 mm) pressure control box ($25 \times 15 \times 12$ cm) that includes a 3D printed gear mechanism (with a gear ratio 8:3) driven by Pololu 50:1 metal gearmotor 37D×70L mm with 64 CPR encoder and Pololu VNH3SP30 motor driver Fig. 2. The pressure sensor (MPX5100DP NXP, Freescale) was mounted on top of the box to continuously measure the growing pressure. The initial pressure of the box was set to 60 kPa, providing sufficient tension for the robot during growth. To prevent explosion when the robot could not grow (or the pressure exceeded the maximum value), we used a safety valve triggered at ≈80 kPa. The unsealed part of the robot was tightly mounted to the pressure box via a 3D printed connector. The pressures of the side actuators were also individually controlled by a proportional valve. Although there is not any feedback from the robot tip, this mechanism utilizes the tension in the backbone and maintains the tension in the spool within a particular range.

C. *Peg board and Gantry*

52 cylindrical pegs (d=8 cm, h=6.5 cm, cut from Kraft mailing tube, Uline) were uniformly distributed on a particle board (120×120 cm) (see Fig. 2). In a hexagonal lattice, the horizontal (d1) and vertical (d2) distances between two neighbor pegs were 18 cm. The side of pegs were covered with a packaging tape to reduce the contact friction with the robot tip. The front side of the pegs were covered with a green colored paper for the image analysis. To easily change the initial position of the robot during the systematic experiments, the pressure box and the robot were mounted on a horizontal gantry (belt driven V-Slot NEMA17 linear actuator bundle, Openbuild), controlled by an Arduino Mega 2560.

D. *Control Board*

The pneumatic control board shown in Fig. 3 consists of two manual pressure regulators, proportional valves, pressure sensors and an Arduino Mega 2560 microcontroller. The manual pressure regulators connected to an air source control maximum pressure of the air passing through the main tube and side sPAMs and are set to 140 kPa and 50 kPa, respectively. The pneumatic tubes (d= 6 mm) and analog pressure sensors (MPX5100DP NXP, Freescale) are connected to the open end of the sPAMs via barbed y-fittings. The pressure of air to the side sPAMs is controlled by the proportional valve (EC-PM-05-4050 EVP, Clippard Incorporated, Cincinnati, OH) operated through an amplifier with a microcontroller. During the experiments the pressure in each sPAMs is regulated by PID control using the feedback from the analog pressure sensors.

III. Experimental Procedure and Results

At the beginning of each experiment, the pressure of the box was set to 60 kPa and the pressure of the sPAMs were set to 30 kPa. For a heterogeneous environment, we used a hexagonal lattice of rigid circular pegs given in Fig. 2 allowing for the possibility of the robot to collide with the

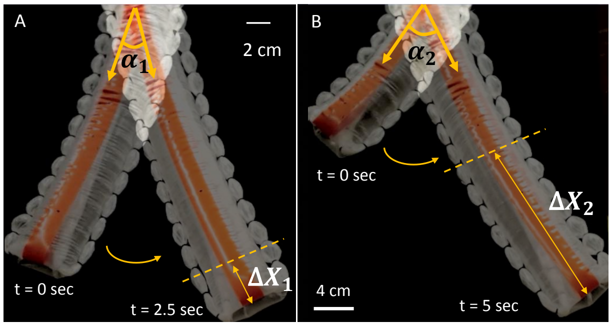

Fig. 5. **Growing and steering in air** to the right with a period of (a) 5 s and (b) 10 s (figures show half cycle). When the sPAMs on the right are activated the robot grows and bends to right during the half period. Images show the bending angle of the tip (a) $\alpha_1 = 35^o$ and (b) $\alpha_2 = 60^o$. The robot tip grows $\Delta X_2 > \Delta X_1$ during half cycle.

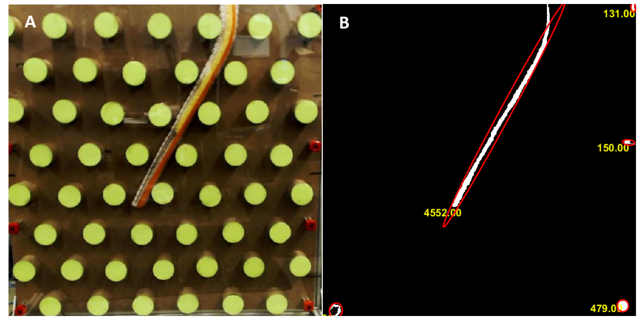

Fig. 6. Example image analyzing using MATLAB Image Processing and Computer Vision Toolbox. Color threshold applied to video frame and the maximum area of the white pixels calculated by MATLAB built-in function *regionprops*.

obstacles causing it to stop its growth (and thus progress through the lattice). The robot began its growth about 10 cm above the first row of obstacles. The locomotion through the obstacle lattice was monitored using a Logitech 920 webcam; collected images were used for off-line tip tracking. The experiments were stopped either when the tip was not able to grow more than 5 seconds or when the maximum expansion (about 92 cm) of the robot was achieved.

Figure 4 shows the shape changes of the robot when the main and side tubes are inflated. In Fig. 4A all the tube pressures are set to zero. When the air pressure is applied to the main tube Fig. 4B, it will expand in a forward direction (perpendicular to tip surface) by everting the tube from inside until it hits an obstacle. 2D tip oscillation occurs by inflating sPAMs arranged on two sides of the main tube Fig. 4C. Because the initial pressure of the control box is set to a specific value and is not modified during the experiment, as the robot grows the pressure decreases. This pressure drop causes a stiffness difference along the backbone of the robot that has already grown and the part that is close to tip i.e. $k_1 > k_2$; which facilitates tip bending. Since sPAMs also grow with tip eversion, the inflation of sPAMs blocks the path of the material inside the main tube and reduces the speed of growing. This effect is shown in Fig. 5. A large part of the growth happens before the sPAMs are fully inflated and if the period (the duration of one cycle; i.e. tip moves left-right-left) of the oscillation is too short (period = 5s, like in Fig. 5A the tip only bends without growing and the bending angle, α_1, is smaller than the bending angle α_2 of period 10s.

We performed two sets of experiments on the regular obstacle lattice; with a period of 10s and without tip oscillation. The horizontal starting position of the robot was varied from 0 to 90 cm across the top of the lattice in 6 cm increments; at each initial condition we performed a minimum of three experiments. We tracked the robot tip from the video frames (2 frames/s) using MATLAB Image Processing and Computer Vision Toolbox. We first converted RGB images to HSV color space, applied color threshold for the orange tape on the robot body, and replaced each pixel in an image with a black pixel if the image intensity was less than some predefined value Fig. 6. Then we calculated final length (or growth length, GL) of the robot using a built-in function (*regionprops*) of MATLAB.

Through multiple trials starting from the different initial positions on the gantry (showed as red circles in Fig. 2A), we found that increased period of oscillation allowed for deeper penetration of the obstacle lattice independent from the starting point. Fig. 7A-B shows the normalized (with respect to starting x position) trajectory of the robot tip during the trials. The robot was significantly more likely to become pinned to obstacles at the first and second row and unable to grow further ($GL = 21.2 \pm 15.7$ cm) when its tip was not oscillated. With an oscillating tip, the robot can grow further ($GL = 66.8 \pm 23$ cm). Fig. 7C-D shows how often each different growth length in a set of data occurs and the insets show the snapshot from videos of the robot at the most common growth length. Collision of the tip with a series of pegs resembles random behavior due to small deviations in an initial starting point. Since the distribution of pegs follow a hexagonal pattern, with tip oscillation most of the trajectories lead to a “running mode” after touching the pegs at the second row of the lattice as seen in Fig. 7; such running modes are the equivalent to the infinite horizon problem studied in lattice billiard dynamics [15], [16], [17]. The presence of infinite horizons lead to superdiffusive effects in such systems and we posit that results in this community could be of use in future control schemes in our robot.

To test the robustness of the oscillated tip mode, we modified the position of some pegs (red circles in Fig. 8) in the lattice to remove the possibility of running modes. We chose one starting point that is close to the center of the board and performed 15 runs. Despite no sensory feedback, the nutating robot tip was still able to find low-resistance paths and exploit cracks in the environment and grow $GL = 75.9 \pm 15.9$ cm. The most common two trajectories are shown in Fig. 8A and the trajectory of the tip and final growth length are given in Fig. 8B. Future systematic experiments will be conducted with lattices consisting of rougher pegs with different sizes and distributions to explore the robustness of the purely open-loop scheme.

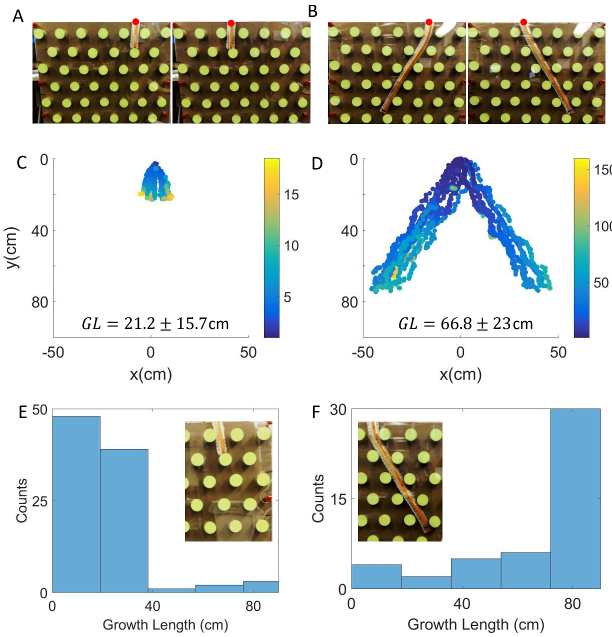

Fig. 7. **Robotic root model navigating a regular obstacle lattice.** Example final growth of the robot starting from different initial position without (A) and with (B) oscillation at the tip. Normalized (with initial starting points) tip trajectories are given in (C-D), color bar represents growth time. Each plot has 21 trajectories that start ± 30 cm from the center of board. The robot can grow a maximum of 92 cm. The histogram of the final growth length (GL) of the robot with and without oscillation at the tip (E, F), insets show zoomed representative images of the robot at the most common growth length. (E) Straight growth without any oscillation at the tip. The mean and standard deviation (std) of the 93 experiments are $GL = 21.2 \pm 15.7$ cm. (F) The tip oscillates with a period of 10 sec, mean and std of the 47 experiments are $GL = 66.8 \pm 23$ cm.

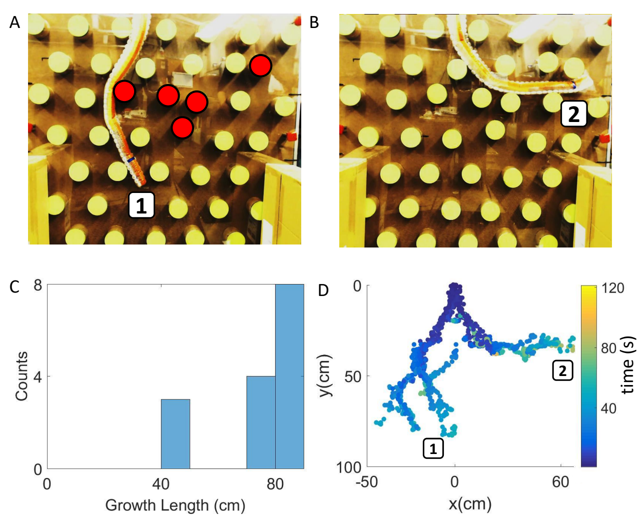

Fig. 8. **Experimental results that show the robustness of tip oscillation on an irregular lattice.** The red pegs were moved to create disturbance on the regular lattice. (A-B) The final two different growing patterns of the robot with an oscillation period 10 s. (C) The histogram of the final growth length ($GL = 75.9 \pm 15.9$ cm) of the robot is given in inset. The most common two trajectories (1 and 2) are given in (A-B), (D) Root tip path of 15 penetration experiments that the robot started from same initial position. Color bar represents time in seconds.

IV. CONCLUSIONS AND FUTURE WORK

In this study we used a root-like growing robot with the ability to steer [9] and showed that emulation of plant root tip oscillation improves the efficacy of autonomous penetration in heterogeneous environments. This movement strategy can be considered to be a beneficial method for exploring *a priori* unknown locations and environments and can be useful in search and rescue operations and medical applications where there is insufficient information about the environment. In future experiments we will investigate the effects of obstacles size, shape, roughness and varying lattice distributions. Further, we will implement a simple feedback controller that leverages the open loop mechanics and dynamics explored in this work. Potentially, such a controller could attain performance matching or possibly exceeding that of a much more complicated feedback controller that is naive to the dynamics and mechanics characterized here.

ACKNOWLEDGMENT

We would like to thank NSF (PoLS SRN, PoLS and Foundation grant 1637446) and Dunn Family Professorship of the School of Physics at Georgia Tech.

REFERENCES

[1] R. R. Murphy, *Disaster Robotics*. The MIT Press, 2014.

[2] M. Travers, J. Whitman, and H. Choset, "Shape-based coordination in locomotion control," *The International Journal of Robotics Research*, vol. 37, no. 10, pp. 1253–1268, 2018. [Online]. Available: https://doi.org/10.1177/0278364918761569

[3] E. W. Hawkes, L. H. Blumenschein, J. D. Greer, and A. M. Okamura, "A soft robot that navigates its environment through growth," *Science Robotics*, vol. 2, no. 8, 2017. [Online]. Available: http://robotics.sciencemag.org/content/2/8/eaan3028

[4] K. R. Lehner, I. Taylor, E. N. McCaskey, R. Jain, P. C. Ronald, D. I. Goldman, and P. N. Benfey, "A histidine kinase gene is required for large radius root tip circumnutation and surface exploration in rice," *bioRxiv*, 2018. [Online]. Available: https://www.biorxiv.org/content/early/2018/10/07/437012

[5] C. Darwin, *The Power of Movement in Plants*, ser. Cambridge Library Collection - Darwin, Evolution and Genetics. Cambridge University Press, 2009.

[6] E. D. Dottore, A. Mondini, A. Sadeghi, V. Mattoli, and B. Mazzolai, "Circumnutations as a penetration strategy in a plant-root-inspired robot," in *2016 IEEE International Conference on Robotics and Automation (ICRA)*, May 2016, pp. 4722–4728.

[7] E. Dottore, A. Mondini, A. Sadeghi, V. Mattoli, and B. Mazzolai, "An efficient soil penetration strategy for explorative robots inspired by plant root circumnutation movements," *Bioinspiration & Biomimetics*, vol. 13, no. 1, p. 015003, 2018. [Online]. Available: http://stacks.iop.org/1748-3190/13/i=1/a=015003

[8] D. Mishima, T. Aoki, e. S. Hirose, Shigeo", H. Asama, E. Prassler, T. Tsubouchi, and S. Thrun, *Development of Pneumatically Controlled Expandable Arm for Search in the Environment with Tight Access*. Berlin, Heidelberg: Springer Berlin Heidelberg, 2006, pp. 509–518.

[9] J. D. Greer, T. K. Morimoto, A. M. Okamura, and E. W. Hawkes, "A soft, steerable continuum robot that grows via tip extension," *Soft Robotics*, vol. 0, no. 0, p. null, 0, pMID: 30339050. [Online]. Available: https://doi.org/10.1089/soro.2018.0034

[10] A. Sadeghi, A. Tonazzin, L. Popova, and B. Mazzolai, "A novel growing device inspired by plant root soil penetration behaviors," *PLOS ONE*, vol. 9, no. 2, pp. 1–10, Feb 2014. [Online]. Available: https://doi.org/10.1371/journal.pone.0090139

[11] J. Aguilar, T. Zhang, F. Qian, M. Kingsbury, B. McInroe, N. Mazouchova, C. Li, R. Maladen, C. Gong, M. Travers, R. L. Hatton, H. Choset, P. B. Umbanhowar, and D. I. Goldman, "A review on locomotion robophysics: the study of movement at the intersection of robotics, soft matter and dynamical systems," *Reports on Progress in Physics*, pp. 1–35, Sep. 2016.

[12] Y. O. Aydin, J. M. Rieser, C. M. Hubicki, W. Savoie, and D. I. Goldman, "6 - physics approaches to natural locomotion: Every robot is an experiment," in *Robotic Systems and Autonomous Platforms*, ser. Woodhead Publishing in Materials, S. M. Walsh and M. S. Strano, Eds. Woodhead Publishing, 2019, pp. 109 – 127. [Online]. Available: http://www.sciencedirect.com/science/article/pii/B9780081022603000068

[13] A. Sadeghi, A. Mondini, and B. Mazzolai, "Toward self-growing soft robots inspired by plant roots and based on additive manufacturing technologies," *Soft Robotics*, vol. 4, no. 3, pp. 211–223, 2017, pMID: 29062628. [Online]. Available: https://doi.org/10.1089/soro.2016.0080

[14] J. D. Greer, T. Morimoto, A. M. Okamura, and E. W. Hawkes, "Series pneumatic artificial muscles (spams) and application to a soft continuum robot," in *2017 IEEE International Conference on Robotics and Automation (ICRA)*, May 2017, pp. 5503–5510.

[15] C. P. Dettmann, "Diffusion in the lorentz gas," *Communications in Theoretical Physics*, vol. 62, no. 4, p. 521, 2014.

[16] P. M. Bleher, "Statistical properties of two-dimensional periodic lorentz gas with infinite horizon," *Journal of Statistical Physics*, vol. 66, no. 1, pp. 315–373, Jan 1992. [Online]. Available: https://doi.org/10.1007/BF01060071

[17] D. N. Armstead, B. R. Hunt, and E. Ott, "Anomalous diffusion in infinite horizon billiards," *Phys. Rev. E*, vol. 67, p. 021110, Feb 2003. [Online]. Available: https://link.aps.org/doi/10.1103/PhysRevE.67.021110